13th World Conference on Earthquake Engineering
Vancouver, B.C., Canada
August 1-6, 2004
Paper No. 2424

STABLE DESIGN OF H_∞ OUTPUT FEEDBACK CONTROL SYSTEMS WITH TIME DELAY

Chi-Chang LIN[1], Chang-Ching CHANG[2], Huang-Lin CHEN[2]

SUMMARY

In this paper, a H_∞ direct output feedback control algorithm through minimizing the entropy, a performance index measuring the tradeoff between H_∞ optimality and H_2 optimality, is developed to reduce the earthquake response of structures. The control forces are obtained from the multiplication of direct output measurements by a pre-calculated time-invariant feedback gain matrix. To achieve optimal control performance and assure control system stability, the strategy to select both control parameters γ and α is extensively investigated considering the control force execution time delay. It is found that the selection of smaller γ or larger α will result in better control performance, but larger control forces requirement. However, a lower bound of γ and an upper bound of α exist. The selection beyond these values will cause the control system instability. For a SDOF damped structure, analytical expressions of direct output feedback gains are derived. It can be proved that the conventional LQR control is a special case of the developed H_∞ control. Direct velocity feedback control is effective in reducing structural responses with much fewer sensors and controllers than the degrees of freedom of the structure. In real active control, control force execution time delay cannot be avoided. Small delay time not only can render the control ineffective, but also may cause the system instability. In this paper, explicit formulas of the maximum allowable delay time and critical control parameters are derived for the design of a stable control system. Some solutions are also proposed to lengthen the maximum allowable delay time.

INTRODUCTION

Since 1970s, remarkable progress has been made in the field of active control of civil engineering structures subjected to environmental loadings such as winds and earthquakes [1]. Among those researches and real applications, various control algorithms have been investigated in designing controllers, for instance LQ [2, 3], LQR optimal control [4, 5] and H_∞ control [6, 7]. The H_∞ control

[1] Dean, *College of Engineering* & Professor, *Department of Civil Engineering, National Chung-Hsing University*, Taichung, Taiwan 40227, R.O.C., Email: cclin3@dragon.nchu.edu.tw, Tel: 886-4-22840438 ext 225, Fax: 886-4-22851992

[2] Graduate Student, *Department of Civil Engineering, National Chung-Hsing University*, Taichung, Taiwan 40227, R.O.C.

theory considers the worst case of external disturbances to design the optimal controller to achieve the desired performance. The results from both numerical simulations and experimental tests indicate that H_∞ control is quite effective [6, 7]. In addition, it had been applied to an actual building in Tokyo using a pair of mass dampers to reduce the bending-torsion motions of the building due to earthquakes [8].

However, there are still many problems that affect active control technique towards large-scale practical application. Time delay and limited number of sensors and controllers are two of these problems. Strictly speaking, a real structure has an infinite number of degrees of freedom (DOFs). It is impossible to acquire full-state measurements and feedback to calculate the required control force. Therefore, a direct output feedback control algorithm becomes necessary from practical point of view. Moreover, in real active control systems, time is consumed in data acquisition, data processing, on-line calculation, and control force execution. There is always a delay between the time at which the control force is assumed to be applied and actually applied, and which may cause degradation in control efficiency or even render the system unstable. Therefore, a robust control with the consideration of time delay effect is necessary. In the literature, the time delay effect on the H_∞ active control system has not been investigated by researchers as much as those on the LQR optimal control [9-11]. Mahmoud et al. [12] designed the H_∞ controller for a class of dynamical systems considering state and input delays. They expressed the control design procedures in the form of linear matrix inequalities. No time-delayed H_∞ output feedback control system was studied.

In this paper, a H_∞ direct output feedback control algorithm through minimizing the entropy, a performance index measuring the trade-off between H_∞ optimality and H_2 optimality, is developed to reduce the structural responses due to seismic loads. To achieve optimal control performance, the strategy to select both control parameters γ and α is extensively studied. The exact solution of output feedback gain for a single-degree-of-freedom (SDOF) damped structure is derived. It can be proved analytically that LQR control is a special case of H_∞ control. Direct velocity feedback control is effective in reducing structural responses with very small number of sensors and controllers compared with the degrees of freedom of the structure. Moreover, explicit formulas are obtained to calculate the maximum allowable delay time to avoid system instability. A formula is also derived to determine the critical control weighting factor of α to assure the system stability. Finally, we propose some solutions to increase the maximum allowable delay time.

H_∞ DIRECT OUTPUT FEEDBACK CONTROL ALGORITHM

The equation of motion of an n-DOF discrete-parameter structure under dynamic loading and active control force can be written as

$$\boldsymbol{M}\ddot{\boldsymbol{x}}(t)+\boldsymbol{C}\dot{\boldsymbol{x}}(t)+\boldsymbol{K}\boldsymbol{x}(t)=\boldsymbol{B_1}\boldsymbol{u}(t)+\boldsymbol{E_1}\boldsymbol{w}(t) \tag{1}$$

where $\boldsymbol{M}$, $\boldsymbol{C}$, $\boldsymbol{K}$ are the $n\times n$ mass, damping and stiffness matrices, respectively. $\boldsymbol{x}(t)$ is the n-dimensional displacement vector, $\boldsymbol{w}(t)$ is the r-dimensional external excitation vector and $\boldsymbol{u}(t)$ is the q-dimensional control force vector. The $n\times q$ matrix $\boldsymbol{B_1}$ and $n\times r$ matrix $\boldsymbol{E_1}$ define the locations of control forces and excitations, respectively.

Represented in state-space form, equation (1) can be rewritten as

$$\dot{\boldsymbol{X}}(t)=\boldsymbol{A}\boldsymbol{X}(t)+\boldsymbol{B}\boldsymbol{u}(t)+\boldsymbol{E}\boldsymbol{w}(t) \tag{2}$$

where

$$\boldsymbol{X}(t)=\begin{Bmatrix}\boldsymbol{x}(t)\\ \dot{\boldsymbol{x}}(t)\end{Bmatrix},\quad \boldsymbol{A}=\begin{bmatrix}\boldsymbol{0} & \boldsymbol{I}\\ -\boldsymbol{M}^{-1}\boldsymbol{K} & -\boldsymbol{M}^{-1}\boldsymbol{C}\end{bmatrix},\quad \boldsymbol{B}=\begin{bmatrix}\boldsymbol{0}\\ \boldsymbol{M}^{-1}\boldsymbol{B_1}\end{bmatrix},\quad \boldsymbol{E}=\begin{bmatrix}\boldsymbol{0}\\ \boldsymbol{M}^{-1}\boldsymbol{E_1}\end{bmatrix}$$

are $2n\times1$ state vector, $2n\times2n$ system matrix, $2n\times q$ controller location matrix and $2n\times r$ external excitations location matrix, respectively. Define a $p\times1$ control output vector $\boldsymbol{Z}(t)$ and a $s\times1$ output measurement vector $\boldsymbol{y}(t)$ as

$$\boldsymbol{Z}(t)=\boldsymbol{C_1}\boldsymbol{X}(t)+\boldsymbol{D}\boldsymbol{u}(t) \tag{3}$$

$$\boldsymbol{y}(t)=\boldsymbol{C_2}\boldsymbol{X}(t) \tag{4}$$

where $\boldsymbol{C_1}$, $\boldsymbol{D}$ and $\boldsymbol{C_2}$ are $p\times2n$, $p\times q$ and $s\times2n$ matrices. In the absence of time delay, the direct output feedback control force is calculated by

$$\boldsymbol{u}(t)=\boldsymbol{G}\,\boldsymbol{y}(t) \tag{5}$$

where $\boldsymbol{G}$ is a $q\times s$ time-invariant feedback gain matrix. According to H_∞ control algorithm, the H_∞ norm of transfer function matrix $\boldsymbol{T_{Zw}}(j\omega)$ of control output with respect to external excitation, takes the form

$$\left\|\boldsymbol{T_{Zw}}(j\omega)\right\|_\infty=\sup\frac{\left\|\boldsymbol{Z}(j\omega)\right\|_2}{\left\|\boldsymbol{w}(j\omega)\right\|_2}<\gamma \tag{6}$$

where $j=\sqrt{-1}$, and sup is defined as the supremum over all $\boldsymbol{w}(t)$; γ is a positive attenuation constant which denotes a measurement of control performance. $\left\|*\right\|_2$ denotes the H_2 norm. From equations (2)-(6), it is derived that the transfer function matrix $\boldsymbol{T_{Zw}}(j\omega)$ is expressed by

$$\boldsymbol{T_{Zw}}(j\omega)=(\boldsymbol{C_1}+\boldsymbol{DGC_2})[j\omega\cdot\boldsymbol{I}-(\boldsymbol{A}+\boldsymbol{BGC_2})]^{-1}\boldsymbol{E} \tag{7}$$

And, the optimal H_∞ controller is designed such that the H_∞ norm of $\boldsymbol{T_{Zw}}(j\omega)$ satisfies the following constraint

$$\left\|\boldsymbol{T_{Zw}}(j\omega)\right\|_\infty=\sup\bar{\sigma}[\boldsymbol{T_{Zw}}(j\omega)]<\gamma \tag{8}$$

where $\sup\bar{\sigma}$ is the largest singular value of $\boldsymbol{T_{Zw}}(j\omega)$. It has been proved [13] that an optimal H_∞ control system is asymptotically stable if there exists a matrix $\boldsymbol{P}\geq0$ that satisfies the following Riccati equation

$$(\boldsymbol{A}+\boldsymbol{BGC_2})^{\mathrm{T}}\boldsymbol{P}+\boldsymbol{P}(\boldsymbol{A}+\boldsymbol{BGC_2})+\frac{1}{\gamma^2}\boldsymbol{PEE}^T\boldsymbol{P}+(\boldsymbol{C_1}+\boldsymbol{DGC_2})^{\mathrm{T}}(\boldsymbol{C_1}+\boldsymbol{DGC_2})=0 \tag{9}$$

The controllers that satisfy equation (8) are not unique and may have an unbounded closed-loop H_2 norm. Thus, one way to design the optimal H_∞ output feedback gain is to solve equation (9) with constraint of the H_2 norm. For example, the so-called combined H_2/H_∞ control problems which the bound of H_∞ norm is imposed and the upper bound of H_2 norm is minimized. Another example is to minimize the Entropy of transfer function $\boldsymbol{T_{Zw}}(j\omega)$

$$E_n(\boldsymbol{T}_{Zw},\gamma)\equiv-\frac{\gamma^2}{2\pi}\int_{-\infty}^{\infty}\ln|\det[\boldsymbol{I}-\gamma^{-2}\boldsymbol{T}^*_{\boldsymbol{Zw}}(j\omega)\boldsymbol{T_{Zw}}(j\omega)]|\,d\omega \tag{10}$$

where $\boldsymbol{T}^*_{\boldsymbol{Zw}}(j\omega)$ is the conjugate transform of $\boldsymbol{T_{Zw}}(j\omega)$. It has been shown that the Entropy of a complex function is an upper bound of its H_2 norm. Therefore, the minimization of Entropy is equivalent to limit the magnitude of H_2 norm. In addition, the Entropy of a function is a useful measurement of how its singular values are close to the upper bound, γ. By minimizing the Entropy, we push all singular values of $\boldsymbol{T_{Zw}}(j\omega)$ away form γ. From the results by Stoorvogel [14], the Entropy is also expressed by

$$E_n(\boldsymbol{T_{Zw}},\gamma)=tr\{\boldsymbol{E}^{\mathrm{T}}\boldsymbol{PE}\} \tag{11}$$

where tr{-} denotes trace of a square matrix. Then, the optimization problem is converted to minimize the Entropy of equation (11) subject to the constraint of equation (9). Incorporated with the constraint, the Lagrangian can be introduced as

$$\begin{aligned}L(\boldsymbol{G},\boldsymbol{P},\boldsymbol{\lambda})\equiv tr\{&\boldsymbol{E}^{\mathrm{T}}\boldsymbol{PE}+\boldsymbol{\lambda}\,[(\boldsymbol{A}+\boldsymbol{BGC_2})^{\mathrm{T}}\boldsymbol{P}+\boldsymbol{P}(\boldsymbol{A}+\boldsymbol{BGC_2})\\&+\frac{1}{\gamma^2}\boldsymbol{PEE}^{\mathrm{T}}\boldsymbol{P}+(\boldsymbol{C_1}+\boldsymbol{DGC_2})^{\mathrm{T}}(\boldsymbol{C_1}+\boldsymbol{DGC_2})]\}\end{aligned} \tag{12}$$

where $\boldsymbol{\lambda}$ is a $2n\times 2n$ Lagrangian multiplier matrix. For simplicity and without loss of generality, let $\boldsymbol{D}^{\mathrm{T}}\boldsymbol{C_1}=0$ and $\boldsymbol{D}^{\mathrm{T}}\boldsymbol{D}=\boldsymbol{I}$, the necessary and sufficient conditions for minimization of $L(\boldsymbol{G},\boldsymbol{P},\boldsymbol{\lambda})$ are

$$(\boldsymbol{A}+\boldsymbol{BGC_2})^{\mathrm{T}}\boldsymbol{P}+\boldsymbol{P}(\boldsymbol{A}+\boldsymbol{BGC_2})+\frac{1}{\gamma^2}\boldsymbol{PEE}^{\mathrm{T}}\boldsymbol{P}+\boldsymbol{C_1}^{\mathrm{T}}\boldsymbol{C_1}+\boldsymbol{C_2}^{\mathrm{T}}\boldsymbol{G}^{\mathrm{T}}\boldsymbol{GC_2}=0 \tag{13a}$$

$$(\boldsymbol{A}+\boldsymbol{BGC_2}+\frac{1}{\gamma^2}\boldsymbol{EE}^{\mathrm{T}}\boldsymbol{P})\boldsymbol{\lambda}+\boldsymbol{\lambda}(\boldsymbol{A}+\boldsymbol{BGC_2}+\frac{1}{\gamma^2}\boldsymbol{EE}^{\mathrm{T}}\boldsymbol{P})^{\mathrm{T}}+\boldsymbol{EE}^{\mathrm{T}}=0 \tag{13b}$$

$$\boldsymbol{B}^{\mathrm{T}}\boldsymbol{P\lambda C_2}^{\mathrm{T}}+\boldsymbol{GC_2\lambda C_2}^{\mathrm{T}}=0 \tag{13c}$$

Thus, the procedures to obtain the H_∞ direct output feedback gain matrix $\boldsymbol{G}$ are: (i) decide a control output vector of equation (3), (ii) select a disturbance attenuation constant γ, (iii) solve equations (13a-13c) to obtain $\boldsymbol{P}$, $\boldsymbol{\lambda}$ and $\boldsymbol{G}$ by any iterative scheme.

According to Yaesh and Shaked [13], the Ricatti equation (9) can be rewritten as

$$\boldsymbol{A}^{\mathrm{T}}\boldsymbol{P}+\boldsymbol{PA}-\boldsymbol{P}(\boldsymbol{BB}^{\mathrm{T}}-\frac{1}{\gamma^2}\boldsymbol{EE}^{\mathrm{T}})\boldsymbol{P}+\boldsymbol{C_1}^{\mathrm{T}}\boldsymbol{C_1}+\boldsymbol{v}^{\mathrm{T}}\boldsymbol{PBB}^{\mathrm{T}}\boldsymbol{Pv}=0 \tag{14}$$

where $\boldsymbol{v}=\boldsymbol{I}-\boldsymbol{\lambda C_2}^{\mathrm{T}}(\boldsymbol{C_2\lambda C_2}^{\mathrm{T}})^{-1}\boldsymbol{C_2}$。 For full-state measurement, $\boldsymbol{C_2}=\boldsymbol{I}$, equations (13a)-(13c) reduce to

$$\boldsymbol{A}^{\mathrm{T}}\boldsymbol{P}+\boldsymbol{PA}+\boldsymbol{P}(\frac{1}{\gamma^2}\boldsymbol{EE}^{\mathrm{T}}-\boldsymbol{BB}^{\mathrm{T}})\boldsymbol{P}+\boldsymbol{C_1}^{\mathrm{T}}\boldsymbol{C_1}=0 \tag{15}$$

which is the same expression derived by Lin and Wei [15] for the H_∞ state feedback control. Thus, direct output feedback control is a general form of the state feedback control. Furthermore, the Entropy is a performance index measuring the trade-off between H_∞ optimality and H_2 optimality. When γ approaches infinity (∞), the Entropy of equation (10) takes the form

$$\lim_{\gamma\to\infty}E_n(\boldsymbol{T_{Zw}},\gamma)=\frac{1}{2\pi}\int_{-\infty}^{\infty}\sum_i\sigma_i^2(\boldsymbol{T_{Zw}}(j\omega))\,d\omega=\|\boldsymbol{T_{Zw}}(j\omega)\|_2^2 \tag{16}$$

and equations (13a)-(13c) reduce to

$$(\boldsymbol{A}+\boldsymbol{BGC_2})^{\mathrm{T}}\boldsymbol{P}+\boldsymbol{P}(\boldsymbol{A}+\boldsymbol{BGC_2})+\boldsymbol{C_1}^{\mathrm{T}}\boldsymbol{C_1}+\boldsymbol{C_2}^{\mathrm{T}}\boldsymbol{G}^{\mathrm{T}}\boldsymbol{GC_2}=0 \tag{17a}$$

$$(\boldsymbol{A}+\boldsymbol{BGC_2})\boldsymbol{\lambda}+\boldsymbol{\lambda}(\boldsymbol{A}+\boldsymbol{BGC_2})^{\mathrm{T}}+\boldsymbol{EE}^{\mathrm{T}}=0 \tag{17b}$$

$$\boldsymbol{B}^{\mathrm{T}}\boldsymbol{P\lambda C_2}^{\mathrm{T}}+\boldsymbol{GC_2\lambda C_2}^{\mathrm{T}}=0 \tag{17c}$$

Above equations have the same forms as those of the optimal LQR direct output feedback control [4]. It shows that the LQR direct output feedback control is a special case of the developed H_∞ direct output feedback control.

Control parameters

Consider a n-story linear shear building equipped with an active tendon control system as shown in Figure 1. The control force $\boldsymbol{u}(t)$ is expressed as

$$\boldsymbol{u}(t) = 4k_c \boldsymbol{U}(t)\cos\theta \tag{18}$$

where $\boldsymbol{U}(t)$ is actuator stroke. k_c and θ are the stiffness and inclination angle of tendons, respectively.

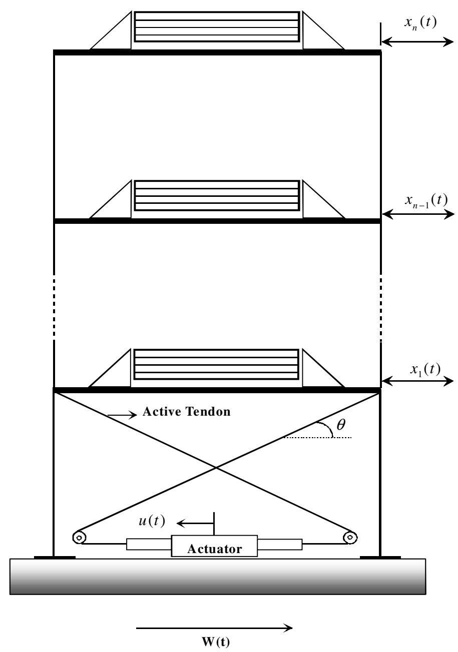

Figure 1. n **-story shear building with active tendon control system**

Define the control output vector satisfying $\boldsymbol{D}^{\mathrm{T}}\boldsymbol{D} = \boldsymbol{I}$ and $\boldsymbol{D}^{\mathrm{T}}\boldsymbol{C}_1 = 0$ as

$$\boldsymbol{Z}(t) = \alpha \begin{bmatrix} \boldsymbol{\Gamma} \\ \boldsymbol{0} \end{bmatrix} \boldsymbol{X}(t) + \begin{bmatrix} \boldsymbol{0} \\ \boldsymbol{I} \end{bmatrix} \boldsymbol{U}(t) \tag{19}$$

Where $\boldsymbol{Z}(t)$ denotes the combination of structural displacement response and actuator stroke and $\boldsymbol{\Gamma}$ is a scalar matrix with element 0 or 1. In equation (19), the control weighting factor, α, determines the relative importance between response reduction and control force requirement. The larger value of α is, the greater reduction of responses. $\alpha = 0$ represents uncontrolled case.

For a SDOF structure with mass m, natural frequency ω_0 and damping ratio ξ_0 as example, $\boldsymbol{\Gamma} = [1 \quad 0]$. The analytical expression of optimal state feedback gain matrix $\boldsymbol{G}$ is obtained by solving equation (15) as

$$\boldsymbol{G} = [\bar{g}_1 \quad \bar{g}_2] = -\frac{4k_c\cos\theta}{m} \cdot [\bar{P}_d \quad \bar{P}_v] \tag{20}$$

And, the controlled frequency, ω_c, and damping ratio, ξ_c, are expressed as

$$\omega_c = \sqrt{\omega_0^{\,2} + P_0^{\,2}\bar{P}_d}\,,\ \xi_c = \frac{2\xi_0\omega_0 + \dfrac{\bar{P}_0^{\,2}}{P_1}(-2\xi_0\omega_0 + \sqrt{4\xi_0^{\,2}\omega_0^{\,2} + 2P_1\bar{P}_d})}{2\sqrt{\omega_0^{\,2} + P_0^{\,2}\bar{P}_d}} \tag{21}$$

where

$$P_0 = \frac{4k_c\cos\theta}{m},\ P_1 = P_0^2 - \frac{1}{\gamma^2},\ \bar{P}_d = \frac{-\omega_0^{\,2} + \sqrt{\omega_0^{\,4} + \alpha^2 P_1}}{P_1},\ \bar{P}_v = \frac{-2\xi_0\omega_0 + \sqrt{4\xi_0^{\,2}\omega_0^{\,2} + 2P_1\bar{P}_d}}{P_1}$$

It is seen from equation (21) that, both control parameters γ and α determine the control performance. $\alpha = 0$ leads to $\boldsymbol{G}$ =0 and $\xi_c = \xi_0$ indicating the uncontrolled case, as expected. As γ decreases or α increases, the controlled damping ratio ξ_c increases. For the extreme case of $\alpha = \infty$, the controlled damping ratio is expressed as $\xi_c = \sqrt{2}/2(P_0/\sqrt{P_1})$ which is a constant value for a chosen γ. At the same time, if $\gamma = \infty$, ξ_c reduces to $\sqrt{2}/2$ (i.e. 70.71%) as obtained by Chung et al. [4] and Lin et al. [11] for the LQR control. This proves that the LQR state feedback control is a special case of the H_∞ state feedback control as $\gamma = \infty$. In addition, under the constraints of $\bar{P}_d$ and $\bar{P}_v$ to be real numbers, and ξ_c less than 100%, the selecting ranges of γ and α are given as

$$\gamma \ge \frac{1}{\sqrt{P_0^2 + \omega_0^4/\alpha^2}} \qquad \text{when } \xi_0 \ge \frac{1}{\sqrt{2}} \tag{22a}$$

$$\gamma \ge \frac{1}{\sqrt{P_0^2 + 4(1-\xi_0^2)\xi_0^2\omega_0^4/\alpha^2}} \qquad \text{when } \xi_0 \le \frac{1}{\sqrt{2}} \tag{22b}$$

Equation (22b) shows that in practice, a minimum value of γ, $\gamma_{\lim}$, exists and takes the form

$$\gamma_{\lim} = \frac{1}{\sqrt{P_0^2 + 4(1-\xi_0^2)\xi_0^2\omega_0^4/\alpha^2}} \tag{23a}$$

Above equation shows that $\gamma_{\lim}$ decreases as α decreases or ω_0 and ξ_0 increase. For the extreme case of $\alpha = 0$, $\gamma_{\lim}$ equals to zero, as expected. However, for a general structure, as $\alpha = \infty$, $\gamma_{\lim}$ equals to a constant as

$$\gamma_{\lim}(\alpha = \infty) = \frac{1}{P_0} = \frac{m}{4k_c\cos\theta} \tag{23b}$$

which depends on the structural system parameters. The stiffer tendon system, the smaller $\gamma_{\lim}$. Moreover, equations (23a) and (23b) reveals that if a γ larger than $\gamma_{\lim}(\alpha = \infty)$ is used, the control system is always stable no matter what α is selected.

Similarly, for only velocity measurement, the analytical expression of direct velocity feedback gain $\boldsymbol{G}$ is obtained by solving equations (13a)-(13c) as

$$\boldsymbol{G} = -\frac{4k_c\cos\theta}{m}[P_v] \tag{24}$$

And, the controlled frequency and damping ratio are expressed as

$$\omega_c = \omega_0,\ \xi_c = \xi_0 + \frac{P_0^2}{P_1}(-\xi_0 + \sqrt{\xi_0^2 + \frac{P_1P_2}{2\omega_0^2}}) \tag{25}$$

In above equations,

$$P_2 = \omega_0^2\gamma^2(1-\sqrt{1-\frac{\alpha^2}{\omega_0^4\gamma^2}}),\ P_v = \frac{-2\xi_0\omega_0 + \sqrt{4\xi_0^2\omega_0^2 + 2P_1P_2}}{P_1}$$

Same as the state feedback control, as γ decreases or α increases, the controlled damping ratio ξ_c increases for direct velocity feedback control. However, due to only velocity feedback, the controlled frequency, ω_c, remains unchanged. From equation (25), it shows that the controlled damping ratio can reach 100%. For the SDOF active tendon control structure, if the desired controlled damping ratio, ξ_{obj}, is given, the required control weighting factor $\alpha_{\gamma,\xi_{obj}}$ can be obtained from equation (25) as

$$\alpha_{\gamma,\xi_{obj}} = \sqrt{2\omega_0^{\,2}\bar{\xi} - \frac{1}{\gamma^2}\bar{\xi}^2} \tag{26}$$

where $\bar{\xi} = \frac{2P_1\omega_0^{\,2}}{P_0^{\,4}}\left(\xi_{obj}-\xi_0\right)^2 + \frac{4\xi_0\omega_0^{\,2}}{P_0^{\,2}}\left(\xi_{obj}-\xi_0\right)$. If $\xi_{obj} = 100\,\%$, the maximum value of $\alpha_{\gamma,100\%}$ can be obtained from equation (26) after determining γ.However, under the constraints of P_2 and P_v to be real numbers and ξ_c less than 100 %, the selecting ranges of γ and α are

$$\omega_0^2\gamma\sqrt{1-(1+\frac{2\xi_0^2}{P_1\gamma^2})^2} \ \le\ \alpha\ \le\ \min[\omega_0^2\gamma,\ \ \sqrt{2\omega_0^2\bar{\xi}_{cr} - \frac{1}{\gamma^2}\bar{\xi}_{cr}^{\ 2}}\,] \quad \text{when}\ \gamma \le \sqrt{1-\xi_0^2}\,/\,P_0 \tag{27a}$$

$$0 \le\ \alpha\ \le\ \min[\omega_0^2\gamma,\ \ \sqrt{2\omega_0^2\bar{\xi}_{cr} - \frac{1}{\gamma^2}\bar{\xi}_{cr}^{\ 2}}\,] \quad \text{when}\ \gamma > \sqrt{1-\xi_0^2}\,/\,P_0 \tag{27b}$$

where $\bar{\xi}_{cr} = \frac{2\omega_0^{\,2}P_1}{P_0^{\,4}}(1-\xi_0)^2 + \frac{4\xi_0\omega_0^{\,2}}{P_0^{\,2}}(1-\xi_0)$.

Based on above derivations and discussions, to achieve optimal control performance and assure control system stability, the appropriate control strategy is to adjust control weighting factor α after the selection of γ based on equations (22) and (27). That makes the selection strategy of control parameters more efficient and flexible.

Numerical simulation

A SDOF structure (S1) which system parameters listed in Table 1 is used for a parametric study to demonstrate the effectiveness of the proposed control algorithm. The analytical and numerical solutions of $\boldsymbol{G}$ and ξ_c of direct velocity feedback (DVF) control for different γ and α are shown in Figure 2. It is seen that the absolute values of $\boldsymbol{G}$ and ξ_c increase dramatically as γ decreases or α increases. The controlled frequency ω_c is always equal to the original natural frequency ω_0. Figure 3 illustrates the transfer function of absolute acceleration with respect to support acceleration for $\gamma = 0.01$ and $\alpha = 0.1,\ 0.5,\text{ and } 1.0$. It is found that the larger α, the smaller peak amplitude of the transfer function. The time histories of acceleration response and control force with ($\alpha = 0.1,\ \ \gamma = 0.01$) and without control under the strong motion part of the free field ground acceleration (EW component) recorded at the campus of National Chung-Hsing University (NCHU) during the 1999 Taiwan Chi-Chi earthquake (Figure 4) are illustrated in Figure 5. Because the system damping ratio increases (from 1.24% to 4.58%), the acceleration response is significantly reduced. It is also seen that the required maximum control force is only 6% of the structural weight.

For a three DOF control structure (S3), which system properties listed in Table 2, the patterns of control force and sensor location are symbolized by F and V. For example, F1V1 indicates that one controller is placed at the first floor and the first floor velocity is measured. The more number of controllers and sensors, the more reduction in structural responses. However, it is found that one pair of collocated controller and sensor at the first floor (F1V1) is effective in significantly increasing all modal dampings and reducing the total structural responses, as illustrated in Table 2 and Figures 6-8 for the case of $\alpha = 0.1$ and $\gamma = 0.1$. The required maximum control force is 11% of structural total weight.

Table 1. System parameters of S1 structure

Mass , m (Kg)	2.9235×10^{3}
Stiffness , k (N/m)	1.3898×10^{6}
Damping , c (N·s/m)	1.5808×10^{3}
Natural frequency , ω_0 (Hz)	3.47
Natural period , T_0 (sec)	0.288
Tendon stiffness , k_c (N/m)	3.721×10^{5}
Tendon inclination , θ (°)	36

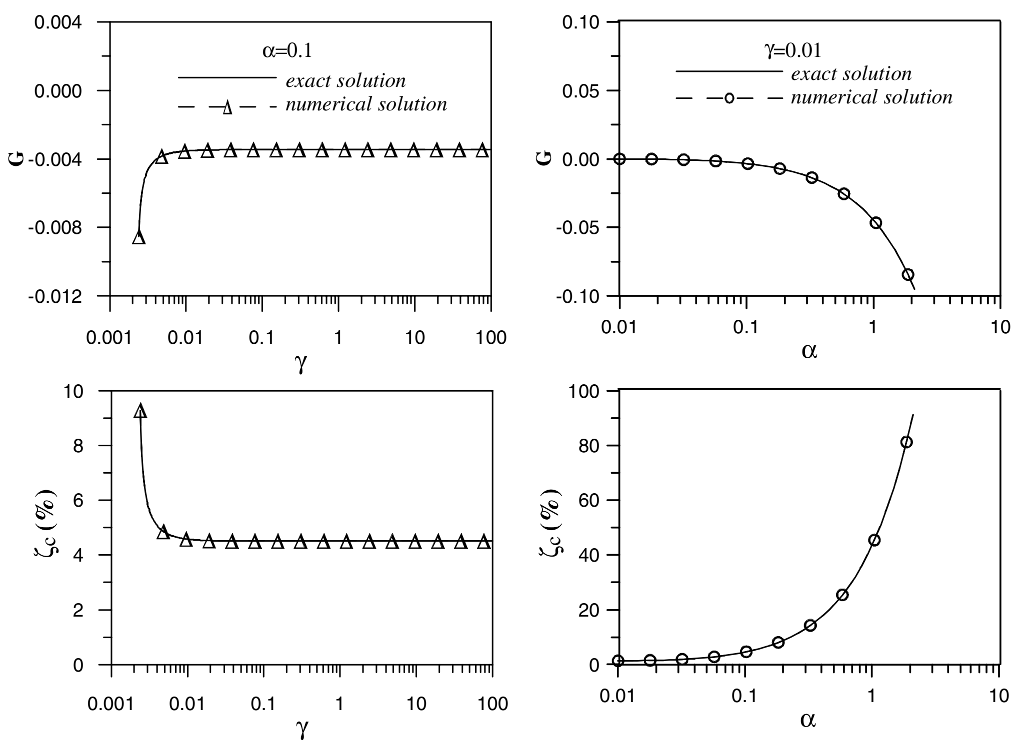

Figure 2. Variation of velocity feedback gain G and controlled damping ratio ξ_c for S1 structure

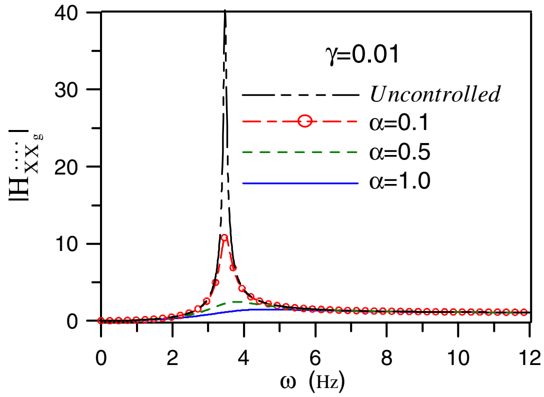

Figure 3. Absolute acceleration transfer function for different α

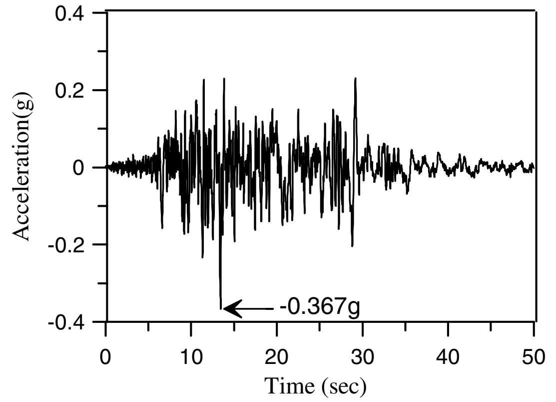

Figure 4. NCHU campus record (EW) of 1999 Taiwan Chi-Chi earthquake

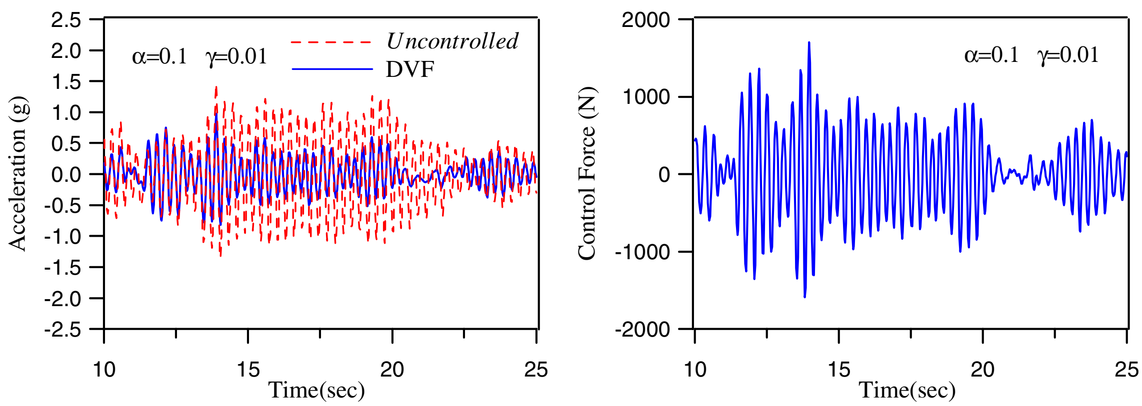

Figure 5. Time histories of acceleration response and control force of S1 structure

Table 2. System parameters of S3 structure with and without control

Mass matrix, $\boldsymbol{M}$ (Kg)	$\begin{bmatrix} 981 & 0 & 0 \\ 0 & 981 & 0 \\ 0 & 0 & 981 \end{bmatrix}$
Stiffness matrix, $\boldsymbol{K}$ (N/m)	$\begin{bmatrix} 2741500 & -1641500 & 369100 \\ -1641500 & 3022000 & -1624700 \\ 369100 & -1624700 & 1333500 \end{bmatrix}$
Damping matrix, $\boldsymbol{C}$ $(\mathrm{N \cdot s/m})$	$\begin{bmatrix} 382.78 & -57.29 & 61.66 \\ -57.29 & 456.89 & -2.63 \\ 61.66 & -2.63 & 437.44 \end{bmatrix}$

Table 2. System parameters of S3 structure with and without control (continued)

	uncontrolled	F1V1 $\alpha=0.1$, $\gamma=0.1$
Natural frequency (Hz)	$\begin{bmatrix}\omega_{1,0}\\ \omega_{2,0}\\ \omega_{3,0}\end{bmatrix}=\begin{bmatrix}2.24\\ 6.80\\ 11.49\end{bmatrix}$	$\begin{bmatrix}\omega_{1,c}\\ \omega_{2,c}\\ \omega_{3,c}\end{bmatrix}=\begin{bmatrix}2.25\\ 6.83\\ 11.38\end{bmatrix}$
Damping ratio (%)	$\begin{bmatrix}\xi_{1,0}\\ \xi_{2,0}\\ \xi_{3,0}\end{bmatrix}=\begin{bmatrix}1.61\\ 0.39\\ 0.36\end{bmatrix}$	$\begin{bmatrix}\xi_{1,c}\\ \xi_{2,c}\\ \xi_{3,c}\end{bmatrix}=\begin{bmatrix}6.16\\ 12.86\\ 4.05\end{bmatrix}$

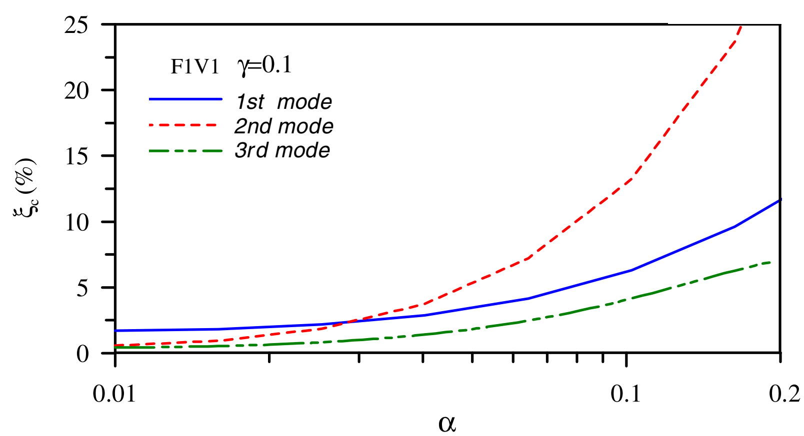

Figure 6. Variation of controlled damping ratio of S3 structure for different α

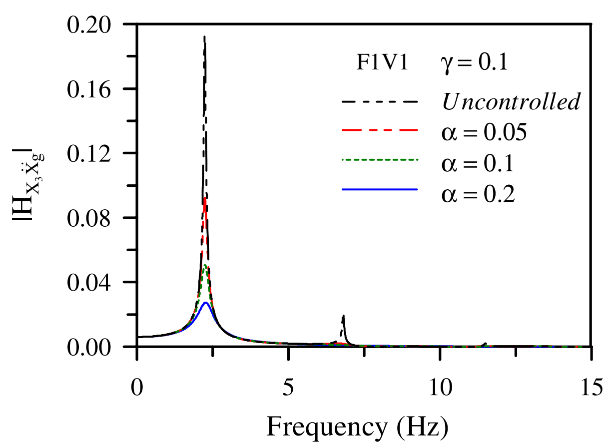

Figure 7. Top floor displacement transfer function of S3 structure for different α

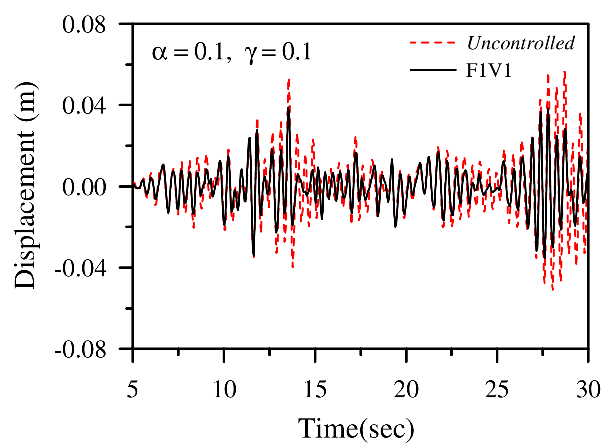

Figure 8. Time histories of top floor displacement response

CONTROL FORCE EXECUTION TIME DELAY

In real active control systems, time is consumed in data acquisition, data processing, on-line calculation, and control force execution. There is always a delay between the time at which the control force is assumed to be applied and really applied. That means the control force at time instant t is expressed as

$$\boldsymbol{u}(t) = 4k_c \cos\theta \boldsymbol{G} \cdot \boldsymbol{y}(t - t_d) \tag{28}$$

where t_d is the delay time. Substituting equation (28) into equations (2) and (3), the system poles or eigenvalues are obtained by solving the following sets of homogeneous algebraic equations

$$\left| \bar{\lambda} \cdot \boldsymbol{I} - (\boldsymbol{A} + e^{-t_d \bar{\lambda}} \cdot \boldsymbol{B} \cdot \boldsymbol{G} \cdot \boldsymbol{C_2}) \right| = 0 \tag{29}$$

where $\boldsymbol{I}$ is the identity matrix and $\bar{\lambda}$ represents complex eigenvalues of the time-delayed control system. The corresponding controlled frequency and damping ratio are given as

$$\omega_c = \left| \bar{\lambda} \right| \quad \xi_c = -\mathrm{Re}(\bar{\lambda}) / \omega_c \tag{30}$$

Where $|-|$ and $\mathrm{Re}\,(-)$ denote absolute value and real part of a complex number, respectively.

For S1 structure with direct velocity feedback, when delay time t_d increases, the controlled damping ratio, ξ_c, varies slightly for small t_d and then drops to zero very fast as shown in Figure 9 for the case of $\gamma = 0.01$ and $\alpha = 0.1,\ 0.5,$ and 1.0. The larger α, the faster degradation of controlled damping. The maximum allowable delay time ($t_{d,\max}$) which causes system instability ($\xi_c = 0$) will also decrease as α increases. As $\gamma = 0.01$, the comparison of $t_{d,\max}$ for state feedback (SFB) and direct velocity feedback (DVF) is given in Table 3. It is found that the smaller α, the longer maximum delay time for both SFB and DVF controls. However, with the same control weighting factor, direct velocity feedback allows longer delay time than state feedback.

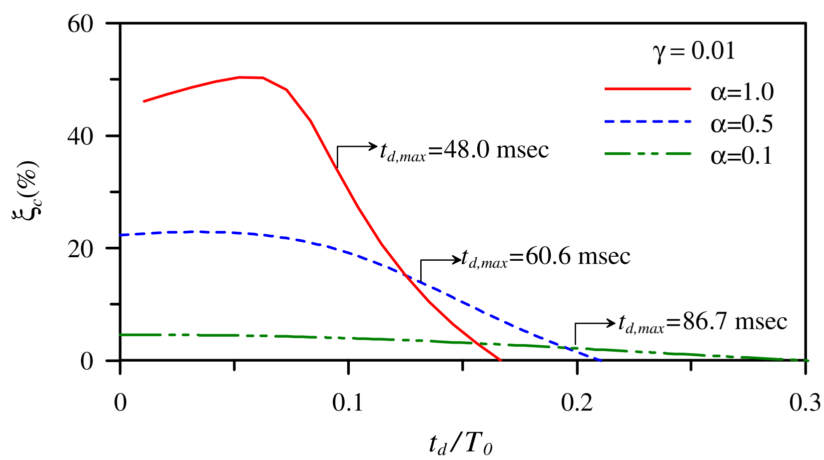

Figure 9. Variation of ξ_c for different t_d / T_0 (S1, DVF)

Similarly, for MDOF control systems with time delay, all modal controlled damping ratios decrease as the delay time or α increases. The higher modal damping ratio reduces faster than those of lower modes. For the S3 structure with F1state and F1V1 controls, the results are given in Table 4 and Table 5. It shows that, when a large α is used, the highest damping ratio, $\xi_{3,0}$, drops to zero first and results in instability of the whole control system for both control types. However, it is also found that, when α is smaller than a certain value, to be determined later, the second modal damping reduces to zero rather than the third and thus, the maximum delay time increases.

Table.3 Maximum delay time of S1 with SFB and DVF controls ($\gamma = 0.01$)

	α=0.1		α=0.5		α=1.0	
	SFB	DVF	SFB	DVF	SFB	DVF
$t_{d,\max}$ (msec)	84.8	86.7	54.2	60.6	40.9	48

Table.4 Controlled results of S3 with F1State control for different α ($\gamma = 0.1$)

	α = 0.05	α = 0.1	α = 0.2	α = 0.5	α = 1.0
$\begin{bmatrix} \xi_{1,c}(\%) \\ \xi_{2,c}(\%) \\ \xi_{3,c}(\%) \end{bmatrix}$	$\begin{bmatrix} 2.80 \\ 0.00 \\ 0.36 \end{bmatrix}$	$\begin{bmatrix} 5.64 \\ 0.00 \\ 0.28 \end{bmatrix}$	$\begin{bmatrix} 11.15 \\ 0.00 \\ 0.10 \end{bmatrix}$	$\begin{bmatrix} 28.31 \\ 3.74 \\ 0.00 \end{bmatrix}$	$\begin{bmatrix} 47.88 \\ 9.24 \\ 0.00 \end{bmatrix}$
$t_{d,\max}$ (msec)	64.2	43.0	36.3	21	16.3

Table.5 Controlled results of S3 with F1V1 control for different α ($\gamma = 0.1$)

	α = 0.02	α = 0.03	α = 0.05	α = 0.1	α = 0.2
$\begin{bmatrix} \xi_{1,c}(\%) \\ \xi_{2,c}(\%) \\ \xi_{3,c}(\%) \end{bmatrix}$	$\begin{bmatrix} 1.88 \\ 0.00 \\ 0.08 \end{bmatrix}$	$\begin{bmatrix} 2.30 \\ 0.97 \\ 0.00 \end{bmatrix}$	$\begin{bmatrix} 3.24 \\ 2.60 \\ 0.00 \end{bmatrix}$	$\begin{bmatrix} 5.74 \\ 6.36 \\ 0.00 \end{bmatrix}$	$\begin{bmatrix} 10.00 \\ 8.27 \\ 0.00 \end{bmatrix}$
$t_{d,\max}$ (msec)	46.9	29.3	24.2	21.5	20

Maximum delay time

For the S1 control structure, the analytical expression of $t_{d,\max}$ for direct velocity feedback control is given as

$$t_{d,\max} = \sqrt{\frac{2}{2\omega_0^2 - 4\omega_0^2\xi_0^2 + P_0^4 P_v^2 - \sqrt{4\omega_0^4 + [2\omega_0^2 - 4\omega_0^2\xi_0^2 + P_0^4 P_v^2]^2}}}\cos^{-1}\left\{\frac{-2\omega_0\xi_0}{P_0^2 P_v}\right\} \tag{31}$$

It is observed that $t_{d,\max}$ increases as system original damping ratio, ξ_0, increases and control weighting factor α decreases as seen in Figure 10. For a damped structure, a critical (or maximum) value of α, $\alpha_{\max}$, exists. When $\alpha < \alpha_{\max}$ is selected, the control system will remain stable even with long delay time.

In addition, as observed previously, the stability of the S3 control system, is generally determined by the third (highest) mode. However, when α decreases or the third original modal damping ratio, $\xi_{3,0}$, increases, the controlled damping ratio of the second or first mode will decrease to zero earlier than that of the third mode. Under this circumstance, $t_{d,\max}$ will thus be increased as seen in Figure 11. This finding eliminates the question that a real structure allows very small delay time because of inherent large frequencies in higher modes, and thus increases the confidence of the application of active control.

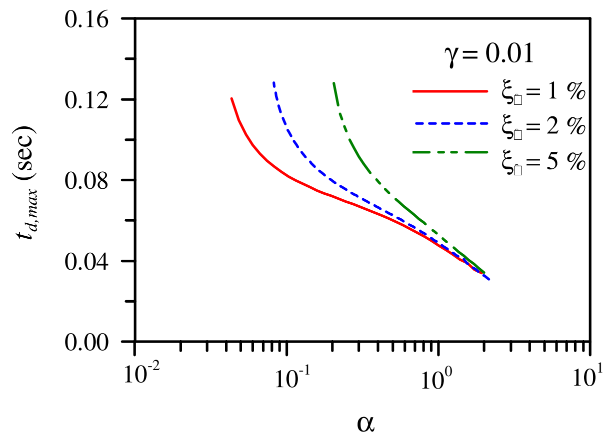

Figure 10. Variation of $t_{d,\max}$ for different α and ξ_0 (S1, DVF)

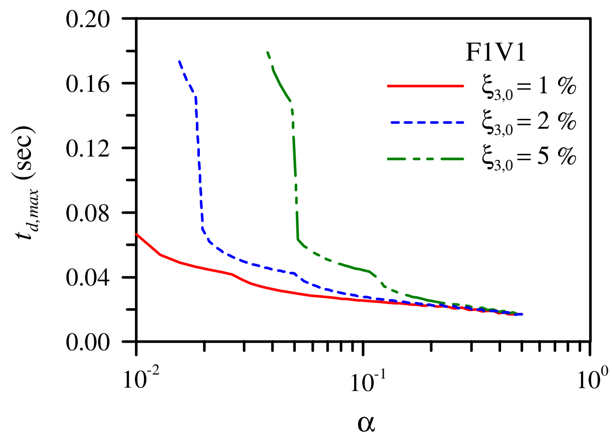

Figure 11. Variation of $t_{d,\max}$ for different α and $\xi_{3,0}$ (S3, F1V1)

Critical control weighting factor

As found in preceding section, the max delay time may be lengthened by selecting appropriate control weighting factors and/or increasing the damping ratio of higher modes. For a given SDOF damped structure, the maximum control weighting factor ($\alpha_{\max}$) exists to satisfy equation (24). That means the value of the function in are cosine equals to minus one, i.e., $(2\omega_0\xi_0)/(P_0{}^2 P_v) = 1$. For the S1 structure with direct velocity feedback, $\alpha_{\max}$ takes the form as

$$\alpha_{\max} = \omega_0^2 \gamma \sqrt{1 - (3 - \frac{2\xi_0}{P_0^2 \omega_0 \gamma^2})^2} \tag{32}$$

which corresponds to $\xi_{c0} = 2\xi_0$. It indicates the control system will always be stable if $\alpha < \alpha_{\max}$ or say $\xi_{c0} < 2\xi_0$. The variation of $\alpha_{\max}$ with different ω_0 or ξ_0 for S1 structure with DVF control is shown in Figure 12. The larger ω_0 or ξ_0 is, the larger α can be used.

For the S3 structure with F1V1 control, the $\alpha_{\max}$ that system stability is dominated by the second mode, versus the third original damping ratio $\xi_{3,0}$ for the third original frequency $\omega_{3,0}$=l, 5, and 10 Hz is shown in Figure 13. $\alpha_{\max}$ increases with the increase of $\omega_{3,0}$ and $\xi_{3,0}$. The larger $\omega_{3,0}$ or $\xi_{3,0}$ is, the larger α can be used. This reconfirms the fact that the stability of MDOF control systems turns to be dominated by lower modes if the higher modes have some dampings for certain value of α.

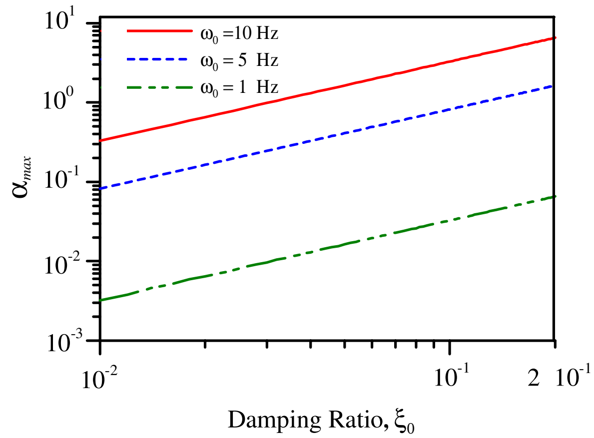

Figure12. Variation of $\alpha_{\max}$ for different ξ_0 and ω_0 (S1, DVF)

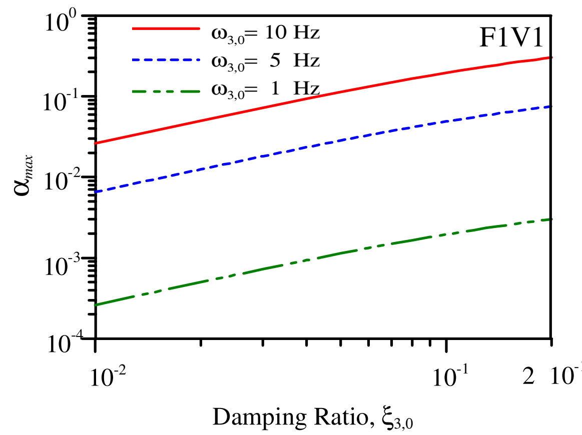

Figure13. Variation of $\alpha_{\max}$ for different $\xi_{3,0}$ and $\omega_{3,0}$ (S3, F1V1)

CONCLUSIONS

This paper develops an optimal H_∞ direct output feedback control algorithm with the consideration of limited number of sensors and controllers and control force execution time delay. The closed form solutions of optimal output feedback control gains, controlled modal frequency and damping ratio are obtained. From the modal parameters, frequency domain and time domain analysis of controlled systems under earthquake excitations, it is demonstrated that one pair of collocated velocity sensor and controller such as F1V1 is sufficient and effective in reducing the dynamic responses of MDOF structures. Analytical expression of control parameter, γ, is also derived to make the control strategy more efficient and flexible. Moreover, the explicit formula is obtained to calculate the maximum allowable delay time. This quantity is a useful parameter for the design of control devices. Finally, the critical control weighting factor is also derived to avoid control system instability. The allowable delay time is lengthened by adding structural dampings through passive dampers and/or selecting a control weighting factor smaller than the critical one. The control performance can thus be significantly improved even with time delay.

ACKNOWLEDGEMENTS

This research was supported in part by Nation Science Council of the Republic of China under the grant No. NSC 92-2211-E-005-032. These supports are greatly appreciated.

REFERENCES

1. Soong TT, Spencer Jr BF. “Active, semi-active and hybrid control of structures”, Proceedings of the 12th World Conference on Earthquake Engineering, Auckland, New Zealand, 2000.
2. Kobori T, Koshika N, Yamada K, Ikeda Y. “Seismic-response-controlled structure with active mass driver system. part 1: design”, Earthquake Engineering and Structural Dynamics 1991; 20: 133-149.

3. Kobori T, Koshika N, Yamada K, Ikeda Y. “Seismic-response-controlled structure with active mass driver system. part 2: verification”, Earthquake Engineering and Structural Dynamics 1991; 20: 151-166.
4. Chung LL, Lin CC, Chu SY. “Optimal direct output feedback of structural control”, Journal of Engineering Mechanics, ASCE 1993; 119: 2157-2173.
5. Lin CC, Chung LL, Lu KH. “Optimal discrete-time structural control using direct output feedback”, Engineering Structures 1996; 18: 472-482.
6. Kose IE, Schmitendorf WE, Yang JN. “ H_∞ active seismic response control using static output feedback”, Journal of Engineering Mechanics , ASCE 1996; 122: 651-659.
7. Chase GJ, Breneman SE, Smith AH. “Robust H_∞ static output feedback control with actuator saturation”, Journal of Engineering Mechanics ASCE, 1999; 125: 225-233.
8. Fujinami T, Saito Y, Morishita M, Koike Y, Tanida K. “A hybird mass damper system controlled by H_∞ control theory for reducing bending-torsion vibration of an actual building”, Earthquake Engineering and Structural Dynamics 2001; 30: 1639-1653.
9. Yang JN, Akbarpour A, Askar G. “Effect of time delay on control of seismic-excited buildings”, Journal of Structural Engineering , ASCE 1990; 116: 2801-2814.
10. Agrawal AK, Fujino Y, Bhartia BK, “Instability due to time delay and its compensation in active control of structures”, Earthquake Engineering and Structural Dynamics 1993; 22: 211-224.
11. Lin CC, Sheu JF, Chu SY, Chung LL. “Time delay effect and its solutions in direct output feedback control of structures”, Earthquake Engineering and Structural Dynamics 1996; 25: 547-559.
12. Mahmoud MS, Terro MJ, Abdel-Rohman M. “An LMI approach to H_∞ -control of time-delay systems for the benchmark problem”, Earthquake Engineering and Structural Dynamics 1998; 27: 957-976.
13. Yaesh I, Shaked U. “Minimum Entropy Static Output-Feedback Control with an H_∞ -Norm Preformance Bound.” IEEE Transactions on Automatic Control 1997; 42(6): 853-858.
14. Stoorvogel AA. “The Singular Minimum Entropy H_∞ Control Problem.” System & Control Letter 1991; 16: 411-422.
15. Lin CC, Wei JY. “Vibration Reduction and Stability Analysis of H_∞ Control Systems”, ASCE, Fourteenth Engineering Mechanics Conference (EM2000), Texas, USA. 2000.